Fermilab

TM-1080
0302.000

Limitations to the Corrections of Orbit Errors Using DC Correction Elements

B.C. Brown and R.K. Rice

December 1981

Abstract

This paper explores the power of a d.c. trim dipole system to correct residual alignment errors in a strong focusing synchrotron. We find that corrections for alignment errors greater than one-half of the beam half width at injection will require aperture during acceleration which is not used by the injected beam. We will discuss the operational effects of large corrections, techniques for studying the problem, and implications for operation of the Fermilab Booster.

Introduction

A standard scheme for orbit correction of a strong focusing synchrotron uses d.c. dipole correction magnets to correct for remanent fields in the magnets and compensates for the misalignment errors by moving gradient (or quadrupole) magnets. Since the remanent fields are unimportant at high fields, one can in principle decouple the corrections by determining misalignments using suitable beam detectors to measure the high momentum closed orbit. Residual small alignment errors can be corrected using the d.c. dipole system. This technique will result in a suitable orbit if the closed orbit measurement is suitably accurate and precise and if the dipole field of the synchrotron is adequately represented by the sum of a constant term (remanent) and a term proportional to current (and thereby momentum).

The trim dipoles are normally adjusted to minimize beam losses and to maximize transmission through the synchrotron. If the high field orbit errors are small enough, the d.c. trim dipoles will be adjusted only to correct the effects of remanent fields and the trim dipole configuration which will minimize beam losses for coasting beam at injection will also maximize the transmission of the synchrotron.

If errors have been made in the high field orbit correction, several undesirable effects will be noted. First, if there are restricted apertures, as there are in any reasonable synchrotron, even if the trim dipoles are adjusted to produce an ideal orbit at injection, when the beam is accelerated, the displacements introduced by the d.c. trim dipoles to correct alignment errors decrease faster than the beam size decreases (p^{-1} vs. $p^{-.5}$). This can lead to beam loss at some intermediate energy by scraping the beam.

Perhaps even more serious is the fact that the motion of the beam centroid during acceleration makes it very difficult to control the betatron frequencies and even the chromaticity if the magnets are imperfect. This can cause beam loss by resonant effects or it can increase the emittance of the beam without necessarily causing beam loss. In addition, it becomes almost impossible to deliver beam with reproducible properties.

Because of serious and fundamental problems with the closed orbit measuring system, the Fermilab Booster has suffered from all of these effects. During the past two years, we have been engaged in a systematic program of reducing the closed orbit errors by a number of indirect measurements of the closed orbit distortions. This paper will discuss the aperture limitations imposed by beam motion when alignment errors are corrected by d.c. trim elements and discuss the diagnostic techniques we have used to improve the Booster orbit[1].

Beam Centroid Motion with D.C. Trim Magnets

It is straightforward to calculate the orbit distortion d(s,p) introduced by a set of trim dipole correction magnets around a synchrotron.

$$d_o(s) = d(s,p_o) = \sum_{\substack{\text{all}\\ \text{dipoles } i}} \frac{[\beta_i \beta(s)]^{1/2} \theta_i(p_o)}{2 \sin \pi\nu} \cos(|\psi_i - \psi(s)| - \pi\nu)$$

where β,ψ are the Courant-Snyder[2] amplitude and phase advance functions, s the location at which the distortion d is found, p_o the injection momentum and ν is the tune. The subscript i designates the correction dipole and Θ_i gives its deflection in radians. Figure 1 gives a plot of such distortions as calculated from the radial corrections used to obtain good transmission in the Booster in May 1981.

This correction will be reduced as the momentum increases

$$d(s,p) = d_o(s) \frac{p_o}{p}$$

To the extent that the dipoles correct for remanent fields, this is desired; however, the correction for misalignment errors are correct at only one energy. In the Booster at present, the effects of remanent fields appear to be small and we neglect them in what follows[3]. This also implies that the orbit distortions at injection which produce good transmission provide an approximate measure of the magnet misalignment. In the vertical plane we now have our result for the distance of the beam center c(s,p) from the uncorrected orbit

$$c(s,p) = d(s,p) = d_o(s)\,\frac{p_o}{p}$$

In the horizontal plane we must add an additional term arising from a momentum error

$$c(s,p) = d_o(s)\,\frac{p_o}{p} + \eta(s)\,\frac{\delta p}{p}$$

where $\delta p/p$ is determined by the r.f. system. For simplicity we use a form for $\delta p/p$ derived in the Appendix:

$$\frac{\delta p}{p} = \frac{d_{L20}}{\eta_{L20}}\,(1-p_o/p)$$

where η_{L20} and d_{L20} are respectively the momentum offset function and injection orbit distortion at the r.f. radial position probe.

Motion of the Edges and Aperture Limitations

Having calculated the motion of the beam center let us now calculate the movement of the edges during acceleration under the usual assumption of adiabatic damping. The beam half width $w(s,p)$ will be given by

$$w(s,p) = w_o(s)\sqrt{\frac{p_o}{p}} = \sqrt{\frac{\varepsilon\beta(s)p_o}{\pi p}}$$

where ε is the emittance of the beam at injection and

$$w_o(s) = w(s,p_o) = \sqrt{\varepsilon\beta(s)/\pi}$$

The positions of the edges $e\pm(s,p)$ are given by the beam centroid displacement plus or minus the half width

$$e_\pm(s,p) = c(s,p) \pm w(s,p)$$

$$= d_o(s)\,\frac{p_o}{p} \pm w_o(s)\sqrt{\frac{p_o}{p}} + \eta(s)\,\frac{\delta p}{p}$$

Since the center displacement $c(s,p)$ and the width $w(s,p)$ decrease at different rates, we may expect on occasion to find the edges to have extrema other than at injection, i.e., the aperture may be limited at

times after injection. We calculate the extrema of e as a function of p in the usual fashion, finding the condition

$$\pm w_o(s) = -2\sqrt{\frac{p_o}{p}}\,[d_o(s) - \eta(s)\,\frac{d_{L20}}{\eta_{L20}}]$$

when our simplifying assumption for $\frac{\delta p}{p}$ is employed. Note that this will be satisfied for at most one of the two edges of the beam. Solving for p we find

$$\frac{p}{p_o} = [\,\frac{2}{w_o(s)}\{d_o(s) - \eta(s)\frac{d_{L20}}{\eta_{L20}}\}]^2$$

which is only relevant for $p/p_o > 1$ in which case an interesting aperture limitation comes about.

We express this limitation quantitatively as follows: If the beam is large enough, then its edges will always move faster because of the decreasing width than because of the motion of the centroid. The boundary for this condition is given by the requirement

$$w_o(s) = 2\,\{d_o(s) - \eta(s)\,\frac{d_{L20}}{\eta_{L20}}\}$$

or

$$e(s) = \frac{4\pi}{\beta(s)}\,\{d_o(s) - \eta(s)\frac{d_{L20}}{\eta_{L20}}\}^2$$

where $\varepsilon(s)$ gives at each location s, the smallest beam emittance which will satisfy this condition. A plot of this emittance limit can then be used to flag locations at which the beam motion will move edges beyond the aperture required by the injected beam. Figure 2 shows a plot of the emittance limitations so derived from the data used for Figure 1. Note that these points may not represent the aperture limits since there may in fact be available space for the beam beyond the space occupied by the injected beam at that location. (Radially we may also gain some flexibility by r.f. control of the momentum error).

Aperture Scans

To obtain information on the actual aperture available for the beam at injection, we use the correction dipoles to provide local orbit

distortions. In figure 3 we plot charge transmitted (for greater than 100 turns after injection) vs. the magnitude of this local distortion. The distortion required to produce beam loss in each direction and the distortion required to produce zero transmission are marked. If this procedure is carried out for the entire ring starting with all correction dipoles at zero current, an independent measurement of the misalignment distortion can be obtained (subject to the same assumptions that the remanent fields are negligible).

Using data such as Figure 3 we construct Figure 4 in which we plot available aperture by recording the edges of the full transmission and zero transmission region (note that the requirements of injection complicate interpretation of such a plot in the injection area). From these transmission plots we also obtain information on the beam size. Using the typical widths in which the beam falls from 100% to 0% transmission we find a width of 22 mm or an emittance of $\varepsilon_H=16\pi$ mm-mr.

The patterns of available aperture for injected beam can be studied in these plots. In particular, we observe aperture oscillations around the ring characteristic of those from a single distortion elsewhere in the ring ("free oscillation"). These suggested that important improvements might be obtained from a few major realignments from SS12 to SS18 and SS22 to SS24. Radially we also explore the implications of the inevitable beam motion due to momentum errors during acceleration. The locations with large apparent beam width correspond to locations where the aperture scan shows slow falloff between full and no transmission and frequently an additional break point in the curve. These correspond to locations where the aperture restriction is not at the large β locations where the standard scans are made but rather at intermediate locations. This interpretation has been confirmed by scans using alternative local bumps which emphasize the low β locations.

Simulation Programs

By utilizing the information on aperture obtained from the aperture scans and combining it with the information on distortions required for good transmission of the accelerated beam, we have sought to obtain enough information to allow orbit improvements thru gradient magnet moves. To aid evaluation of the data, further calculations have been carried out to simulate beam edges based on injected beam size and adiabatic damping. Figure 5 shows the zero transmission edges from the aperture plot in Figure 4, the distortion plot from Figure 1 and simulated beam edges for a beam of 15 π mm-mr injected emittance. The edges of the injected beam are shown along with the edges at maximum excursion where these lie outside the injected beam envelope. Data in the vertical place are shown in Fig. 6. Using these and other graphic techniques we have sought to evaluate both the technique and the data.

We have evaluated the consistency of the data sets (where errors are introduced by problems such as varying injection conditions) in order to best achieve orbit corrections. The distortion data and the aperture scan data provide independent information, although both are interpreted with the same assumption on remanent fields. The apparent difference in radial centerline shown in Fig. 5 is due to a slightly different guide field setting used during the two measurements.

If aperture limitations were always given by mechanical obstructions the picture given by the above aperture scans could perhaps be complete and sufficient. In fact, the aperture limits in Booster are more typically bad field regions in the magnets. Non-linearities introduced by these fields combined with space charge tune shift effects make details of further simulations complicated. For this reason as well as the problems of detailed consistency of the data, we have not carried this simulation effort further at this time.

Conclusions

Quantitative limitations on the performance of a d.c. correction element system have been found and related to the corrections required for operation of the Fermilab Booster. Our result shows that for corrections larger than one half the injected beam size, the beam occupies aperture after injection which is not required for the injected beam. We observed problems of beam loss well after injection in the areas indicated by this analysis. Efforts are underway to correct this problem by improved orbit alignment and will be reported elsewhere.

Acknowledgements

We gratefully acknowledge the help and guidance of Curt Owen in suggesting the problem, working out the procedure and preparing this document. The realignment project has been carried out by the entire Booster Group Staff with help of a summer student A. Oliver and John Crawford of the Operations Group. D. Edwards and C. Ankenbrandt have greatly aided by review of the manuscript.

References

1. Earlier related work on the Booster aperture is reported in B.C. Brown et al., Design of an Additional Extraction/Injection Area for the Fermilab Booster, IEEE Trans. on Nucl. Sci., NS-26 , 3173 (1979) and C.W. Owen et al., Status of Efforts to Improve the Transverse Properties of the Fermilab Booster, IEEE Trans. of Nucl. Sci., NS-28 , 2907 (1981).

2. Courant and Snyder, Annals of Physics 3 , 1 (1958).

3. To generalize our results one can consider them to apply to that portion of the correction field due to the misalignment.

4. For details see, R. Webber, Local Orbit Bumps in Booster, Fermilab Operations Bulletin No. 627, 1978.

Appendix

Since we use a single radial pick-up [at Booster Long Straight Section 20] to control the radial feedback system we can write

$$\frac{\delta p}{p} = \frac{-1}{\eta_{L20}} \left(d(s_{L20},p) - \sigma(p) \right)$$

where $\sigma(p)$ is an offset function put into the feedback system to control the average radius. Since

$$d(s_{L20},p) = d_{L20} \frac{p_o}{p}$$

where $d_{L20}=d(s_{L20},p_o)$ we find

$$c(s,p) = d_o(s) \frac{p_o}{p} - \frac{\eta(s)}{\eta_{L20}} d_{L20} \frac{p_o}{p} + \frac{\eta(s)}{\eta_{L20}} \sigma(p)$$

where the result is now valid in both horizontal and vertical planes if we suitably set $\eta=0$ for the vertical. If we choose to hold fixed the radius at the r.f. detector (as one simple case) then $\sigma(p)=d_{L20}$ and

$$\eta_{L20} \frac{\delta p}{p} = d_{L20} \left(1-p_o/p\right)$$

Figure Captions

1. Closed orbit distortion around Booster Ring produced at injection momentum by the d.c. dipole corrections used to produce good transmission during operation in May 1981.

2. Smallest emittance beam which at any point allows accelerated beam to stay within envelope of injected beam as both beam size and orbit distortions decrease. The line with * represents the calculation in

the text while the unmarked line represents a calculation ignoring the $\delta p/p$ term.

3. Typical aperture scan showing charge transmission for first 300 μsec. (100 turns) vs. beam position as determined by 3 magnet dipole bump currents. Note edges marked of full and zero transmission regions.

4. Aperture scan data for horizontal plane of Booster showing full and zero transmission edges of the beam. The data for Booster periods 24 and 1 are distorted by the requirements of injecting onto the orbit and may give center line information but no aperture information.

5. Zero transmission aperture of the Booster as measured June 1981 is compared to orbit distortion from Fig. 1. Simulated beam edges for injected beam and edges at maximum excursion are shown. Beam emittance of 15 π mm-mr is assumed.

6. Same as Figure 5 but for vertical plane. Emittance of 8 π mm-mr is assumed.

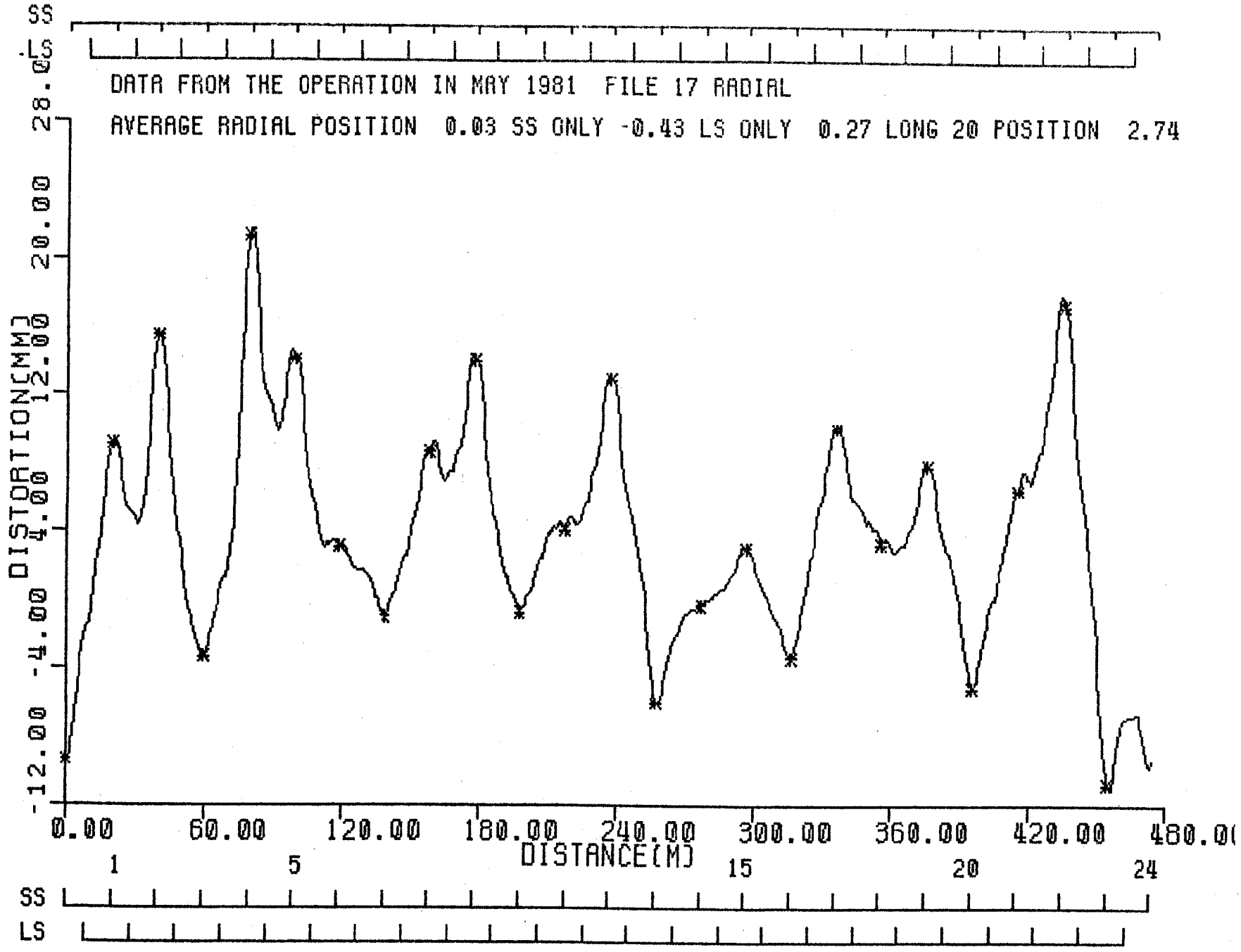
SS
LS
DATA FROM THE OPERATION IN MAY 1981 FILE 17 RADIAL
AVERAGE RADIAL POSITION 0.03 SS ONLY -0.43 LS ONLY 0.27 LONG 20 POSITION 2.74
DISTORTION[MM]
28.00
20.00
12.00
4.00
-4.00
-12.00
0.00
60.00
120.00
180.00
240.00
300.00
360.00
420.00
480.00
DISTANCE[M]
1
5
15
20
24
SS
LS

FIGURE 1.

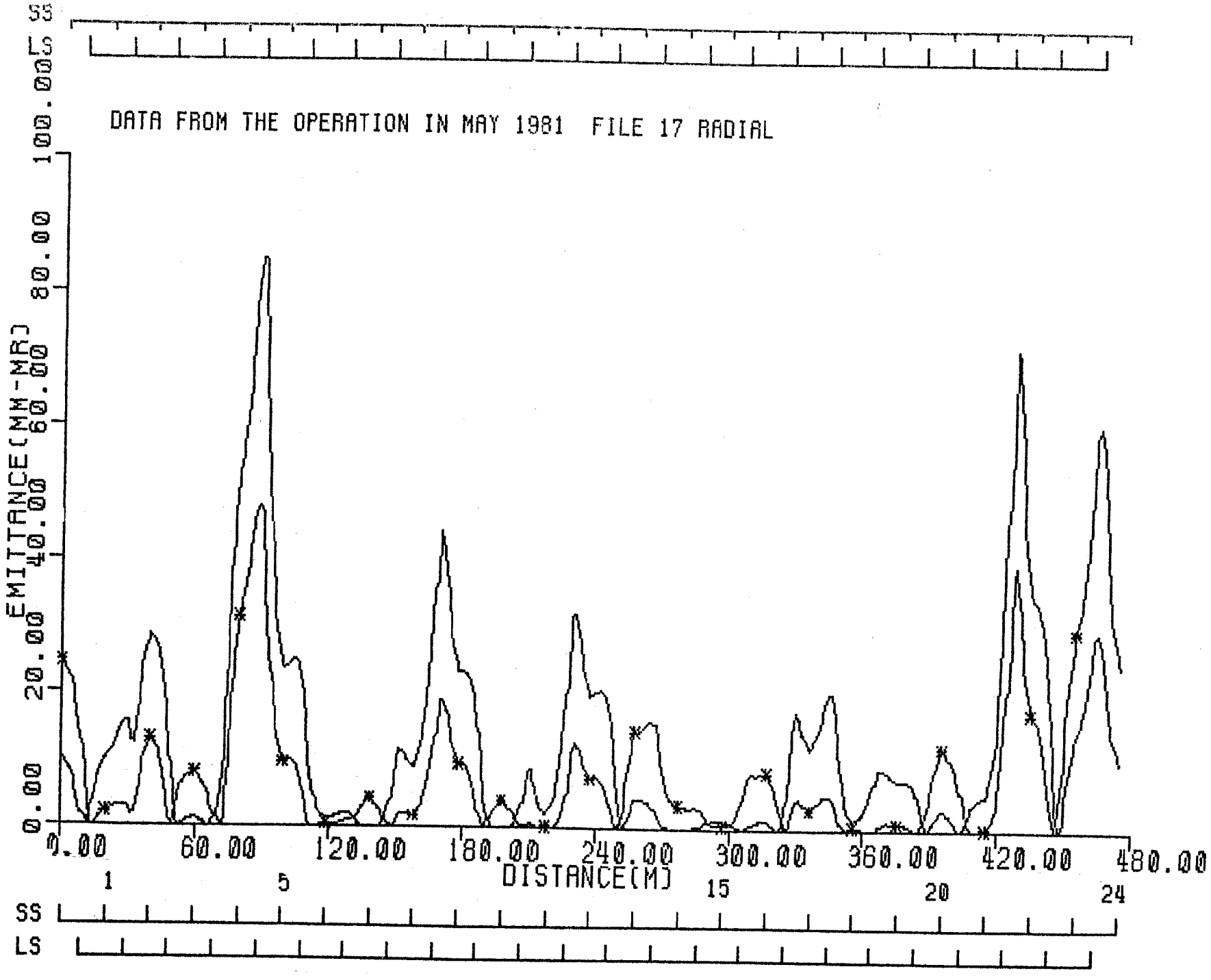
SS
LS
DATA FROM THE OPERATION IN MAY 1981 FILE 17 RADIAL
EMITTANCE[MM-MR]
100.00
80.00
60.00
40.00
20.00
0.00
0.00
60.00
120.00
180.00
240.00
300.00
360.00
420.00
480.00
DISTANCE[M]
1
5
15
20
24
SS
LS

FIGURE 2.

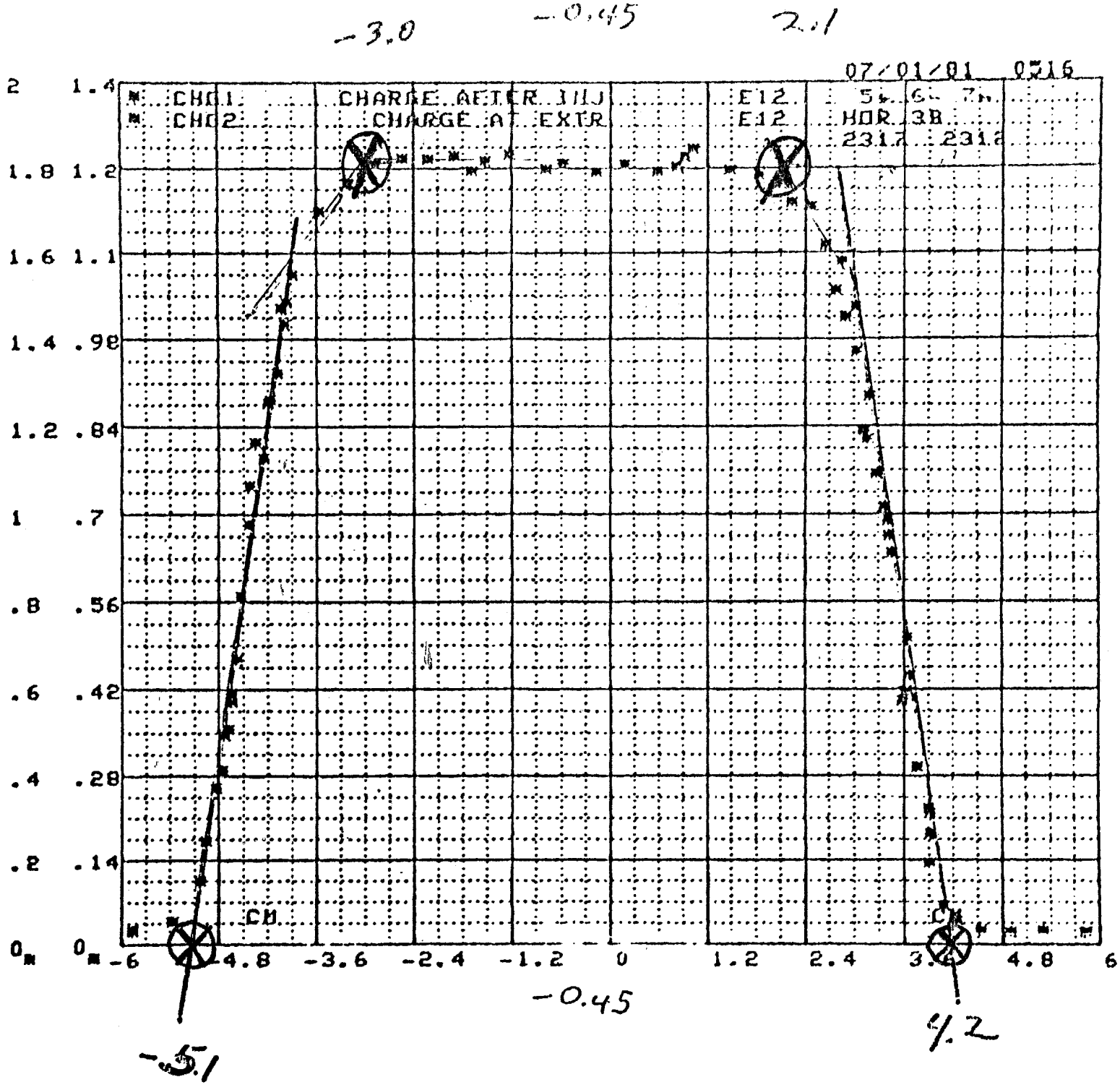
-3.0
-0.45
2.1
07/01/81 0716
CH1 CHARGE AFTER INJ
CH2 CHARGE AT EXTR
E12
E12 HOR 3B
2317 2318
CH
CH
-0.45
-5.1
4.2

FIGURE 3

FIGURE 4

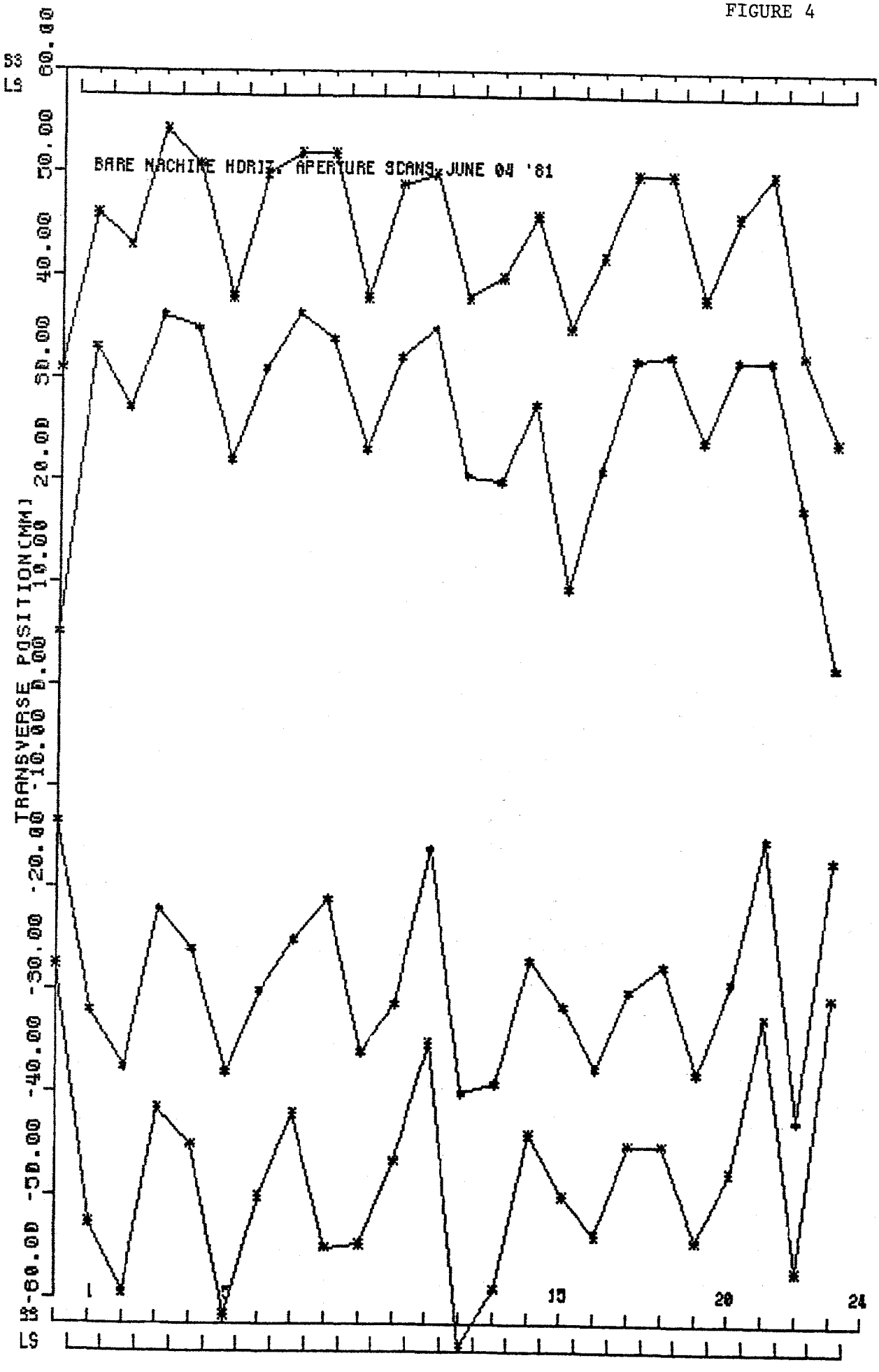
BARE MACHINE HORIZ. APERTURE SCANS, JUNE 04 '81
TRANSVERSE POSITION(MM)
60.00
50.00
40.00
30.00
20.00
10.00
0.00
-10.00
-20.00
-30.00
-40.00
-50.00
-60.00
1
15
20
24
SS
LS

FIGURE 5

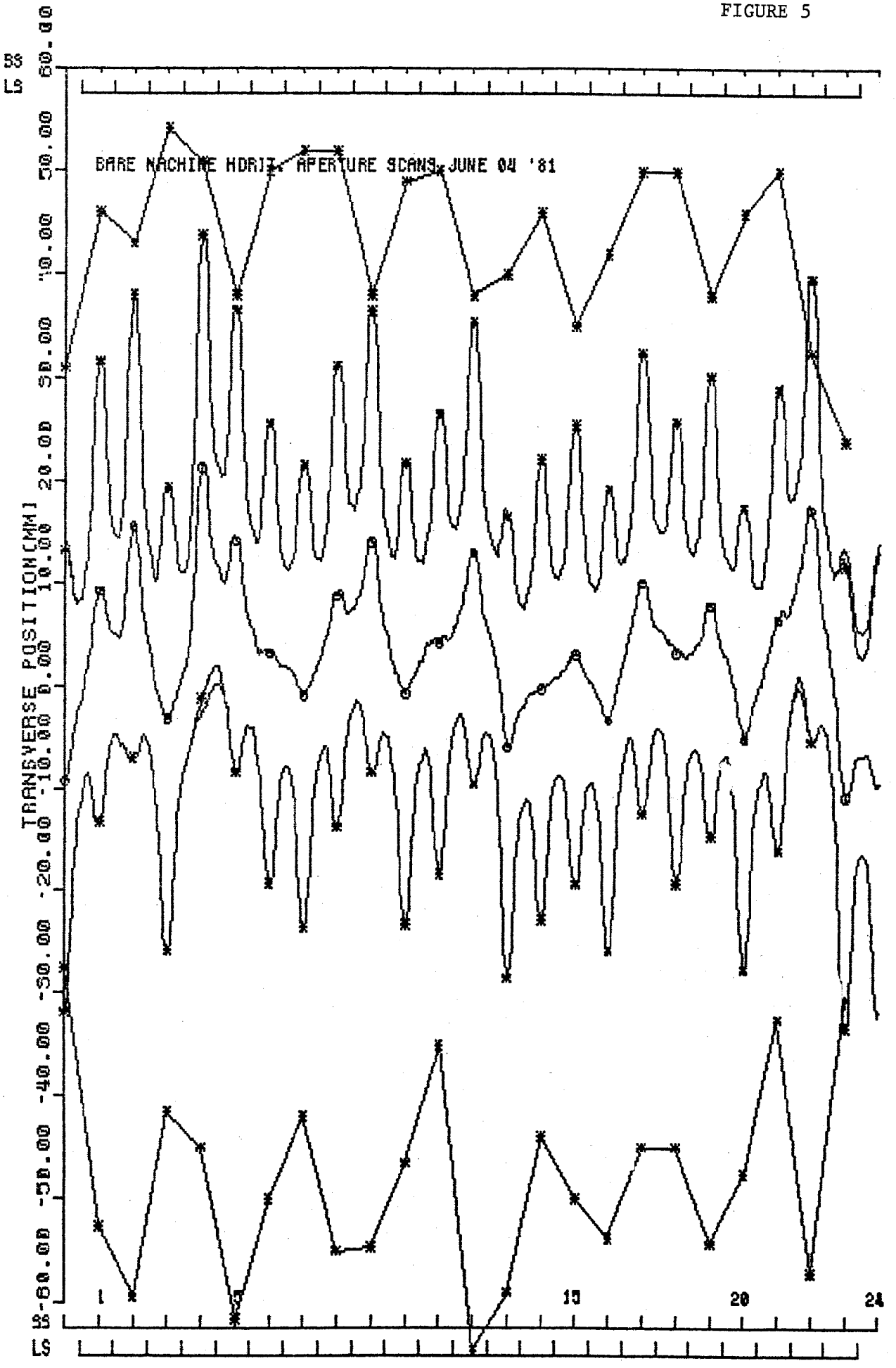
BARE MACHINE HORIZ. APERTURE SCANS JUNE 04 '81
TRANSVERSE POSITION(MM)
60.00
50.00
40.00
30.00
20.00
10.00
0.00
-10.00
-20.00
-30.00
-40.00
-50.00
-60.00
1
5
10
15
20
24
SS
LS

FIGURE 6

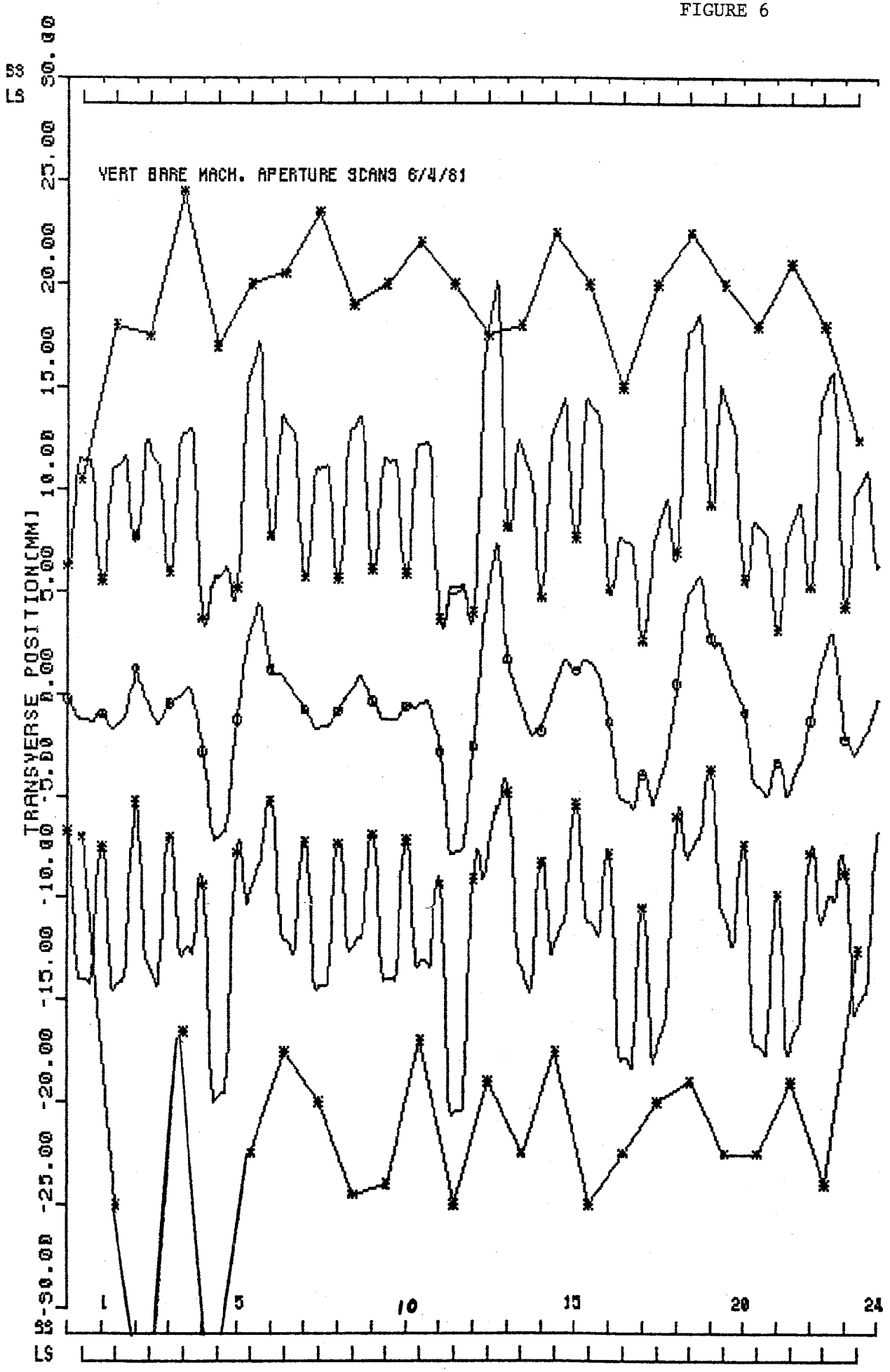
VERT BARE MACH. APERTURE SCANS 6/4/81
TRANSVERSE POSITION[MM]
30.00
25.00
20.00
15.00
10.00
5.00
0.00
-5.00
-10.00
-15.00
-20.00
-25.00
-30.00
1
5
10
15
20
24